JOURNAL OF MATERIALS SCIENCE 5 (1970) 283–294

On Continuum Models of Ductile Fracture

W. W. GERBERICH
College of Engineering, University of California, Berkeley, California, USA

Several fracture criteria are reviewed with respect to ductile fracture. It is suggested that both critical crack-tip displacement, $2V_c^*$, and critical fracture strain, ϵ^*, criteria may describe the fracture of a ductile second phase rod in a ductile matrix. As a first approximation, this is experimentally verified by observations of ductile stainless steel fibres fracturing in an age-hardened aluminium matrix. For 0.05, 0.10 and 0.20 volume fraction composites, the average fracture strains are calculated to be 1.15 as compared to a measured average of 0.93 while the average critical crack-tip displacement is calculated to be 0.50 mm as compared to an "observed" average of 0.40 mm. The statistical variation in the fracture strain was not sufficiently small to allow any choice between these proposed criteria. In fact, both the experimental and theoretical evidence point to the equivalency of these criteria as given by

$$2V_c^* = \pi l^* \epsilon^*$$

where l^* is the microstructural unit in front of the crack over which the strain is greater than or equal to ϵ^*.

1. Introduction

Many continuum approaches to fracture have been developed in the last twenty years including stress concentration, stress intensity and strain energy release rate (modified Griffith) concepts. However, there has been limited use of these in the understanding of how to make materials more resistant to fracture. For this reason, one of the most promising areas is that of applying continuum mechanics and continuous dislocation distribution theory to the vicinity of the crack, in the region where the microstructural constituents control fracture nucleation and growth. Two such developments are the crack-tip displacement concepts as espoused by Cottrell [1], Wells [2] and Tetelman and McEvily [3] and the ductile fracture concepts of McClintock *et al* [4, 5]. The former describes the fracture process in terms of a "micro-tensile" sample fracturing at the crack-tip while the latter describes ductile shear fracture in terms of a hole-coalescence theory.

It is the purpose of this paper, first, to develop in a very simple way some of the current ductile-fracture concepts and then attempt to test these concepts using some experimental evidence obtained from crack propagation studies of a fibre-reinforced composite. A composite system was used so that the unit over which fracture took place would be unambiguous and so that the flow and fracture characteristics of the individual components could be characterised. All of these values are necessary but not readily attainable in the study of homogeneous materials. Therefore, the composite system was utilised so that various ductile-fracture criteria could be properly assessed. The experimental study includes the detection of the fracture history of stainless steel fibres in an aluminium matrix by an acoustic emission technique; metallographic analysis of fracture strains involved in fibre fracture; and stress-intensity analysis of crack-propagation characteristics.

2. Theoretical Background

Many contemporary fracture concepts have their roots based in the energy balance concept originally derived by Griffith [6] to explain fracture phenomena in glass. He assumed that spontaneous fracture would occur when the

total energy of the system was unchanged by small variations of the crack length, i.e.

$$\frac{\partial(U+V)}{\partial C}=0 \tag{1}$$

where U is the change in the strain energy of the system with a flaw, V is the potential energy of creating new fracture surfaces and $2C$ is the major axis of an elliptical crack.** For essentially brittle materials such as glass, the energy associated with creating new surfaces is the surface tension, γ_s. Without stating the details, which have been reiterated many times elsewhere, e.g. [3, 7], equation 1 leads to

$$\sigma=\left[\frac{2E\gamma_s}{\pi C}\right]^{\frac{1}{2}} \tag{2}$$

where σ is the applied stress and E is the tensile modulus of elasticity. For materials that do not behave elastically or have atomically sharp cracks, it is appropriate to modify equation 2. First consider the crack-tip radius effect. Tetelman and Johnston [8] have interpreted Orowan's [9] analysis to show that

$$\sigma=\left[\frac{2E\gamma_s}{\pi C}\frac{\rho}{a_0}\right]^{\frac{1}{2}} \tag{3}$$

where ρ is the crack-tip radius and a_0 is the atomic spacing. Although the justification of equation 3 for plastically deforming materials might be argued on theoretical grounds, it nevertheless gives a useful qualitative interpretation of the crack-tip radius effect. If some mechanism such as chemical dissolution blunts the crack-tip, the stress which can be maintained prior to catastrophic fracture increases. Next, consider inelastic behaviour. Orowan [9] and Irwin [10] interpreted Griffith's equation for metals in terms of the plastic energy absorption, γ_p, occurring during crack extension. Instead of γ_s controlling, there is a combined term, $\gamma_m=\gamma_s+\gamma_p$, which is substituted in equation 2 for γ_s. In the notation of Irwin who defines the critical parameter as the strain energy release rate, G,

$$G=2\gamma_m=\frac{\sigma^2\pi C}{E}. \tag{4}$$

Combining equations 3 and 4, it is seen that

$$G=2\gamma_s\frac{\rho}{a_0}, \tag{5}$$

which indicates that the actual value controlling fracture increases with ρ/a_0. As this interpretation is based upon an extension of elastic analyses, it would seem to be quantitatively suspect when $\rho \gg a_0$ (e.g. 10^4a_0) which is the case for many reasonably tough materials.

A second approach which may have more applicability to ductile-fracture is the crack-tip displacement concept. It has been proposed [1, 3] that slow crack growth advances by the fracturing of "micro-tensile" samples at the crack-tip. The length of the sample is limited by the root radius of the crack and the width is limited by those microstructural factors which limit ductility. Since the gauge length of the sample would be nearly equal to the diameter of the crack-tip, 2ρ, the crack-tip displacement is given by

$$2v_C=2\rho\epsilon \tag{6}$$

where ϵ is the strain adjacent to the crack front. This, then, leads to a failure criterion [1, 3] when the strain reaches the fracture ductility, ϵ^*,

$$2v_C^*=2\rho\epsilon^* \tag{7}$$

Taking the fracture strain to be exceeded over the dimensions of the micro-tensile sample, one can easily visualise a brittle second phase rod fracturing ahead of the main crack. Alternatively, a ductile rod at the crack-tip could be visualised to neck down considerably prior to fracture. For applied stresses up to about 60% of the yield strength, σ_{ys}, the crack-tip displacement is given by [11]

$$2v_C=\frac{\pi\sigma^2C}{\sigma_{ys}E}. \tag{8}$$

From equations 4 and 8, it is seen that

$$2v_C=\frac{G}{\sigma_{ys}}. \tag{9}$$

which demonstrates the relationship between crack-tip displacement and the strain energy release rate. Consider this with respect to the point of fracture. If one stretches the applicability of the Griffith approach and the crack-tip displacement approach to a single system, then combining equations 5, 7 and 9 and eliminating ρ gives

$$\gamma_s=\sigma_{ys}\epsilon^*a_0. \tag{10}$$

The physical interpretation of this is that in truly brittle materials if the yield strength reaches the theoretical strength of the solid and

**A complete list of symbols used in this paper appears following the Appendix.

the fracture strain is exceeded only over the atomic spacing, then $\epsilon^* a_0$ is equivalent to the crack-tip displacement, i.e. the strain times the gauge length. It is obvious then that equations 5 and 7 are not compatible if sufficient micro-yielding occurs prior to fracture. This has been pointed out by Tetelman and McEvily [3] who relegate equation 5 to those systems where continuous cleavage may proceed with stresses at the crack-tip at the theoretical limit.

Cottrell [1] has generalised the crack-tip displacement concept in terms of the work of fracture per unit fracture area. In terms of the displacement, $2v_C$, and stress, σ_C, at the crack-tip, the work is given by

$$2\gamma = 2\int_0^\infty \sigma_C \, dv \, . \tag{11}$$

Cottrell proposed a rectilinear approximation to the law of force so that at fracture, equation 11 becomes

$$2\gamma = 2\sigma_C v_C^* \, . \tag{12}$$

For elastic behaviour, $2v_C^*$ is the atomic dimension and the stress at the crack-tip, σ_C, is the theoretical strength or about $E/5$, giving

$$\gamma_s = 0.1 \, Ea_0 \tag{12a}$$

which is in reasonable agreement with measured values of γ_s. For plastic behaviour, $2v_C^*$ is related to the crack-tip radius and fracture strain by equation 7 and σ_C is the yield strength giving

$$2\gamma_m = G = \sigma_{ys} \, 2v_C^* = 2\sigma_{ys}\rho\epsilon^* \, . \tag{12b}$$

Physically, this demonstrates that the larger the critical crack-tip displacement and, as a result, the larger the crack-tip radius and fracture strain that can be sustained prior to catastrophic failure, the larger the energy absorption.

A criticism of both the energy or crack-tip displacement approaches can be made in that there has been no explicit microstructural size-factor involved in any of the equations proposed thus far. For example, what are the relative contributions of large particles with good ductility as compared to small particles with poor ductility? In order to make an unambiguous comparison, simultaneous consideration of both size and ductility effects is needed. McClintock *et al* [4, 5] have taken such a detailed approach for ductile fracture by a hole-growth mechanism.

In a more general way, McClintock and Irwin [12] have derived the criterion for fracture under anti-plane strain behaviour to be

$$K_{IIIC} = \tau_{ys}[\pi l^* \xi^*/\xi_y]^{\frac{1}{2}} \tag{13}$$

where τ_{ys} is the shear yield strength; ξ^* is the shear strain at fracture; ξ_y is the elastic shear strain; l^* is the microstructural unit over which the fracture strain is exceeded; and K_{IIIC} is the critical value of the mode III stress intensity factor related to strain energy release rate, G_{III}, and shear modulus, μ, by

$$K_{III} = [2\mu G_{III}]^{\frac{1}{2}} \, . \tag{13a}$$

It can be seen that there is some microstructural unit, l^*, over which the fracture strain is exceeded, causing crack growth to occur at the condition, K_{IIIC}.

Similarly, a tensile fracture criterion can be made by using analogous strain distributions, stresses and strains. Gerberich [13] has demonstrated that the analogy to the mode III strain distribution also approximates that for a crack under tensile loading, giving

$$\epsilon_1 = \frac{\sigma_{ys} R_p}{El} \tag{14}$$

where ϵ_1 is the maximum principal strain, R_p is the plastic zone diameter and l is the distance in front of the crack-tip. McClintock [14] has suggested that R_p be given in terms of the mode I stress intensity factor by

$$R_p = \frac{K_I^2}{\pi \sigma_{ys}^2} \tag{15}$$

where K_I is related to the mode I strain energy release rate** by

$$K_I = [EG_I]^{\frac{1}{2}} \tag{15a}$$

Again, assuming that the fracture strain is exceeded over l^* so that $\epsilon_1 \geqslant \epsilon^*$, a combination of equations 14 and 15 give

$$K_{IC} = [\pi \sigma_{ys} El^* \epsilon^*]^{\frac{1}{2}} \, . \tag{16}$$

This failure criterion is schematically shown for a ductile rod in fig. 1. It is now useful to consider how these concepts might apply to the observations made on a unidirectional composite where the "microstructural" size and ductility factors are known.

**This is for plane stress conditions. For plane strain considerations, the right-hand side of equation 15a must be multiplied by $(1/1 - \upsilon^2)^{\frac{1}{2}}$, where υ is Poisson's ratio.

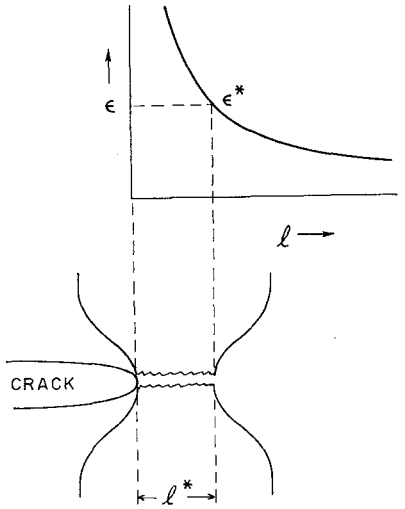

Figure 1 Concept of critical fracture strain ahead of the crack.

3. Experimental Approach

In order to test a ductile-fracture criterion, it was necessary to have both a ductile matrix and a ductile fibre so that relative strength and ductility characteristics could be evaluated.

3.1. Material Selection

One such material system consists of ductile steel fibres in aluminium where diffusion-bonding does not significantly degrade the mechanical properties of the fibres. As such a composite could be purchased commercially, 2.54 mm thick plates with volume fractions of 0.05, 0.10, 0.20 and 0.40 were obtained.** The particular composites evaluated were made up of the following constituents:

wt %	C	Mo	Ni	Cr	Mn	Si	Fe	Cu	Zn	Mg
N355 stainless steel (0.23 mm diameter)	0.13	2.85	4.5	15.5	0.75	0.35	bal.			
2024-T4 aluminium							0.1	0.6	0.5	0.5	4.4	0.25	1.5

Preparation of the composites was essentially by hot-pressing layups at about 500° C in a 1000 ton hydraulic press. Afterwards, the aluminium was aged to the T4 condition. Cross-sections of three volume fractions are shown in fig. 2. It is seen that a relatively uniform spacing of fibres was attained with little void content in the matrix.

3.2. Technique for Measuring Stress Intensity

Single-edge notch specimens were utilised to study a crack growing across the fibres. A crack-line loaded sample was chosen since this provides about a 10:1 mechanical advantage with respect to failing the specimen in uniaxial tension. For this reason, there is no danger of failing the specimen at the loading-pin holes. The specimen configuration, which was essentially 51 mm wide by 76 mm high, is indicated in fig. 3. Knowing the load (P) the specimen thickness (B) width (W) and crack length (C), the stress intensity can be determined from

$$K = \frac{P}{BW^{\frac{1}{2}}} \mathrm{f}\left(\frac{C}{W}\right) \tag{17}$$

where $\mathrm{f}(C/W)$ as given in fig. 3 is taken from the numerical solution of Srawley and Gross [15]. The height of the specimen was not always the same because of shortage of material, but W/H_p did stay within the limits indicated in fig. 3. Specimens were pulled at a crosshead speed of 0.1 cm min^{-1} and load-time recordings were made to maximum load, at which point specimens were unloaded for metallographic examination.

3.3. Technique for Measuring Elastic Waves

During the crack-propagation tests, a technique for monitoring discontinuous crack growth was utilised. This technique is based upon the detection of elastic waves associated with the energy release of a crack jump. Detection of such stress-wave emission (SWE) as connected with discontinuous crack motion has been accomplished under conditions of rising load [16], stress-corrosion-cracking [17], and spontaneous strain-ageing embrittlement [18]. Essentially, a SWE is converted to an electrical signal by a piezoelectric crystal which may be mounted directly to the specimen or be contained in an attached transducer such as an accelerometer. For the relatively large SWE expected in the present study, an accelerometer transducer was utilised, as indicated schematically in fig. 4. The voltage signal from the acceleratometer is amplified by the charge amplifier, filtered to cut out extraneous mechanical noises, further amplified to drive a damped galvanometer with high frequency response, and directly recorded on an oscillograph. In this way, it was anticipated that the large SWE associated with fibre fracture could be used to determine the exact load at which fibre breaks occurred.

**Harvey Aluminium Company, Torrance, California.

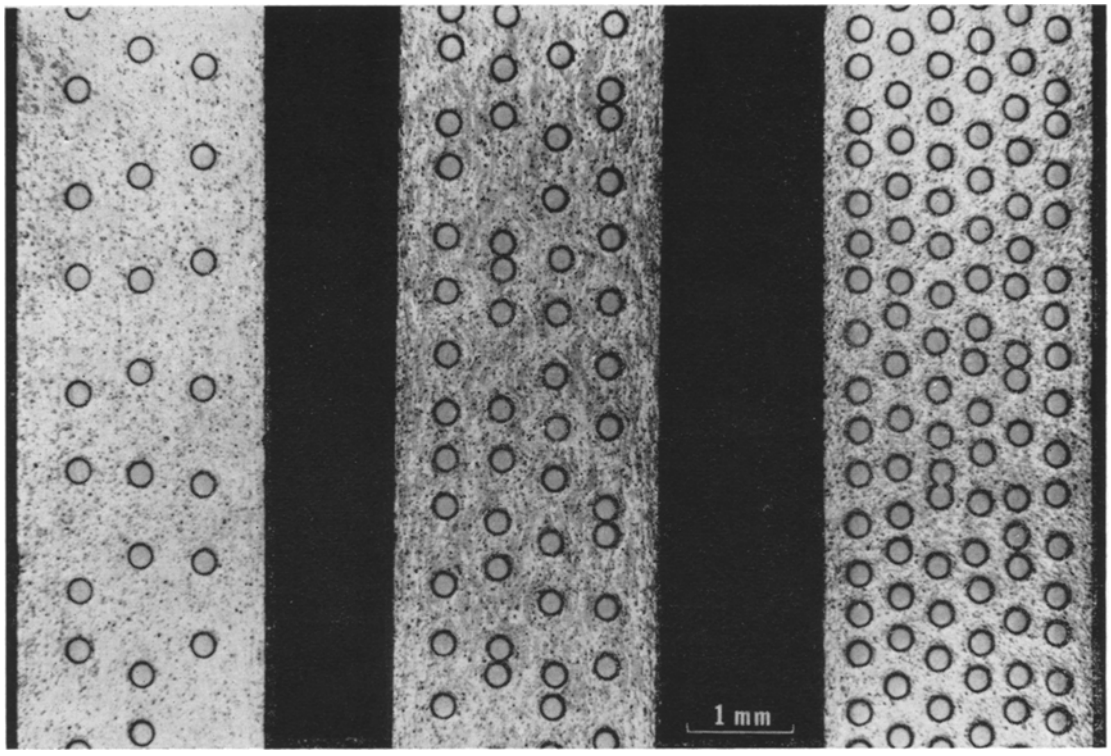

Figure 2 Cross-sections of 0.05, 0.10 and 0.20 volume fraction composites.

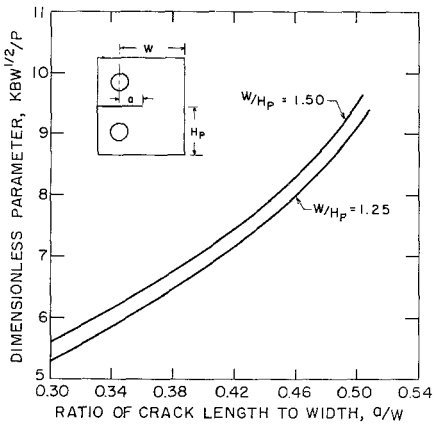

Figure 3 Specimen configuration and numerical solution for stress-intensity factor of notched specimens.

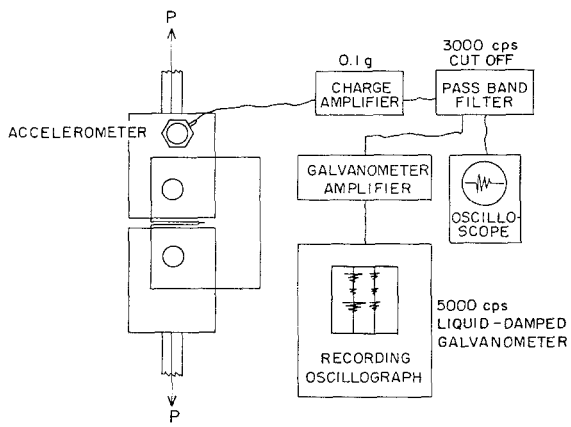

Figure 4 Set-up for recording emitted stress waves.

3.4. Metallographic Technique

After the test, the fracture path was studied by sectioning the partially cracked fracture specimens. As the specimens were unloaded somewhat after maximum load but prior to total failure, the orientation and position of the crack-tip with respect to the ductile fibres was obtained. Also possible was an estimate of the fracture ductility since the necking profile of the fractured fibres gives a measured fracture strain from

$$\epsilon_f = \ln \frac{A_0}{A_f} \tag{18}$$

where A_0 and A_f refer to original and final cross-sectional areas of the fibres. For these measurements, some of the polishing planes were not mid-thickness and care was taken to reconstruct profiles so that reasonable estimates of fracture strains could be made. Additional confirmation of the fracture strains was desired and so one 0.20 volume fraction specimen was pulled to complete fracture. The fracture surface was then examined with a JEOLCO JSM-1 scanning electron microscope operated at 25 kV in the secondary electron mode.

4. Results and Discussion

From the uniaxial tensile and crack-propagation data obtained on these unidirectional composites, it was possible to test the several fracture criteria under discussion.

4.1. Uniaxial Behaviour

Mechanical properties of the individual constituents are given in the following tabulation:

	Modulus of elasticity, kg mm^{-2}	Poisson's ratio	Yield strength, kg mm^{-2}	Ultimate strength, kg mm^{-2}
Stainless steel fibres	21×10^3	~0.3	302	315
2024-T aluminium	7.3×10^3	0.33	35	47.5

The stainless steel results represent the average of 10 fibres extracted from 0.10 and 0.20 volume fractions while the aluminium data are nominal values taken from the literature. The ultimate tensile strength data conformed to a rule of mixtures, which, in terms of a perfectly elastic-plastic matrix, is given by

$$\sigma_{comp} = \sigma_{mys} V_m + \sigma_f V_f , \qquad (19)$$

where σ are stresses, V are volume fractions, m and f denote fibre and matrix, and ys denotes yield strength. However, if some strain-hardening in the matrix occurs and the total plastic strain at fracture is considerable, then a closer estimate might be

$$\sigma_{comp} = \sigma_{m\,UTS} V_m + \sigma_f V_f , \qquad (20)$$

where UTS denotes ultimate tensile strength. These two relationships are seen to represent the lower and upper bounds for the observed behaviour in fig. 5.

4.2. Fracture Behaviour

The answers to two questions were necessary if any description of the fracture process were to be meaningful with respect to establishing a failure criterion. First, the load and crack length associated with each fibre fracture were needed so that a stress intensity level could be determined for each fibre break. Secondly, it was necessary to know the position of the advancing crack with respect to the fibre break and the critical fracture strain involved in that fibre break. The first question was answered using the acoustic emission technique while the second was investigated via metallography and scanning electron microscopy.

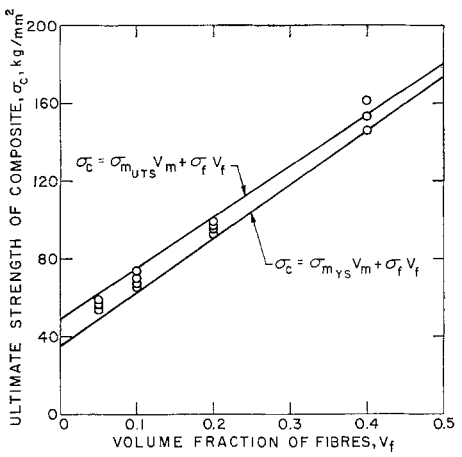

Figure 5 Effect of volume fraction on ultimate strength of composites.

4.2.1. SWE Observations

Monitoring the crack propagation tests with the acoustic emission technique allowed pinpointing of the fibre breaks. Two examples of the SWE associated with crack propagation across steel and boron fibres in metal-matrix composites are shown in fig. 6.** Noting the slight differences in time scale, there are at least an order of magnitude more SWE's emanating from the fracture of boron fibres. Although this is partly due to the fact that there were about twice as many boron fibres per unit fracture area, it can mostly be attributed to multiple breaks (5 to 10 typically) in the boron fibres as compared to single breaks in the steel ones.

Further correlation of SWE to stainless-steel fibre fracture was obtained by comparing the load drops occurring during fibre fracture to the stress waves. As noted in fig. 7, each load drop was coincident with the occurrence of a large SWE. In some instances, two SWE's

**Testing of aluminium-boron composites is in the initial stages and is not reported except for this one result which is for comparative purposes.

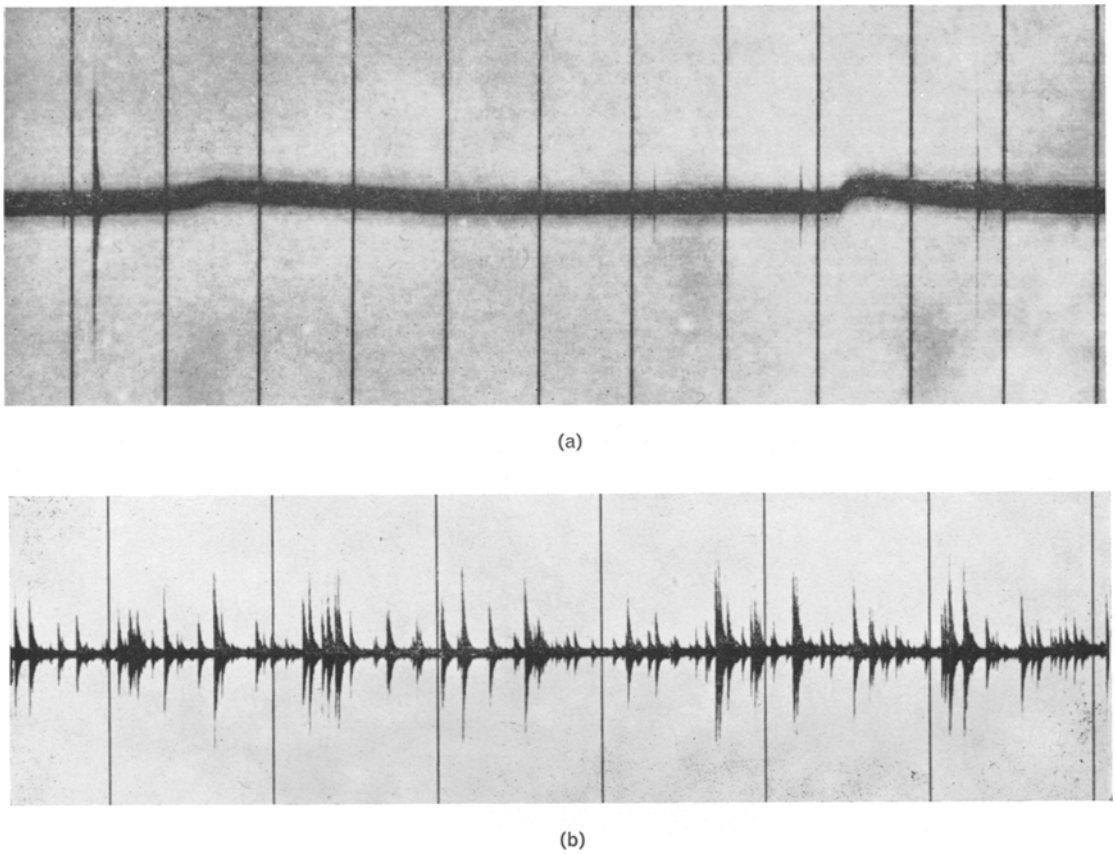

Figure 6 Typical stress waves emitted during crack propagation across unidirectional fibrous composites. Top: SWE from steel fibres; bottom: SWE from boron fibres. 1 sec/division.

occurred almost simultaneously which indicated two fibres fracturing even though the load only dropped once. For two specimens with 10% volume fraction, metallographic sectioning indicated a total of fifty-four fractured fibres while SWE observations indicated a total of fifty-two. The excellent correlation between these emitted waves and the fibre fracture allowed determination of the time of failure of the fibres. That is, the load for the first fibre fracture and the initial crack length were used in equation 17 to determine K. Subsequent rows of fibre fracture allowed K to be calculated from the appropriate load and crack length represented by the initial crack plus the number of inter-fibre spacings over which the crack had travelled. This permitted an average load and hence an average stress intensity factor to be associated with fibre fracture. For example, in one specimen with a volume fraction of 0.10, K ranged from 249 to 303 kg mm$^{-\frac{3}{2}}$ for fibre fracture.

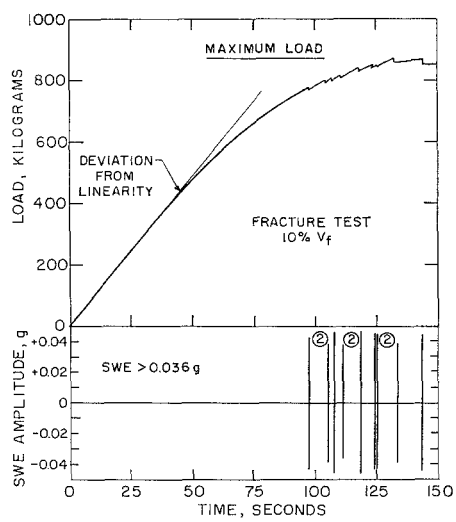

Figure 7 Comparison of stress waves to load drops observed during crack extensions in 0.10 volume fraction composite.

Similar calculations for 0.05 and 0.20 volume fraction composites were made, all of the results being given in table I. It is seen that the stress intensity for fibre fracture increases with volume fraction. In fact, K is nearly proportional to $(V_f)^{\frac{1}{2}}$ which has a theoretical basis as discussed below.

4.2.2. Microscopic Observations

Examples of fractures are shown for three different volume fractions in fig. 8. It was observed that the crack would progress in the matrix; a fibre would fracture; the matrix would crack again and then another fibre would fracture. Although it is not obvious in the micrographs, there is a crack in the matrix between the 1st and 2nd fibres for the 0.05 volume fraction; between the 3rd and 4th fibres for the 0.10 volume fraction; and between the 1st and 2nd fibres for the 0.20 volume fraction specimens. Thus, it was assumed that as the crack arrived at the matrix-fibre interface, the fracture of the fibre necessitated that the fracture strain be exceeded over the entire fibre diameter. Since the fibres necked considerably before the fracture, the average neck diameter was taken as the value of l^* over which the fracture strain had to be exceeded, as was depicted in fig. 1. The value of l^* was measured from the photomicrographs and is given in table I for each volume fraction.

From the micrographs, the true fracture strain was also measured, the values as determined from equation 18 being given in table I. Although there may be some variation with volume fraction, the average fracture strain of 0.93 for twenty-one fibres reasonably describes most of the data. To further verify the fracture strain, scanning microscopy gave additional results on seven fibres, a typical micrograph being shown in fig. 9. The fracture strain was determined as ranging from 0.60 to 1.05 with the average being 0.84 for this 0.20 volume fraction specimen. As this is in good agreement with the average value of 0.77 for 0.20 volume fraction data taken from table I, it may be assumed that the rest of the observations are reasonably accurate. Nevertheless, it would appear that there is a statistical variation of about a factor of two in the observed fracture strains.

4.2.3. Fracture Criteria

In the theoretical development, two fracture criteria are suggested for ductile fracture, a crack-tip displacement concept and a critical fracture strain concept. Consider first the fracture strain criterion. Values of ϵ^* may be calculated from equation 16 from the observed value of K for fibre fracture as taken from the SWE data, and the experimental values for σ_{ys}, E and l^*. From the data in table I, calculated values of ϵ^* are shown to agree approximately with measured values of ϵ_f in table II. It should be noted that in this calculation the value for E used in equation 16 was the secondary modulus of elasticity, E_C', which is the appropriate value for a two-phase system in which the fibre is elastic and the matrix is yielding at the "apparent" elastic-plastic boundary. Rice [20] has shown that in the small volume of material adjacent to the crack, the fracture criterion is dependent upon the unloading path. With these

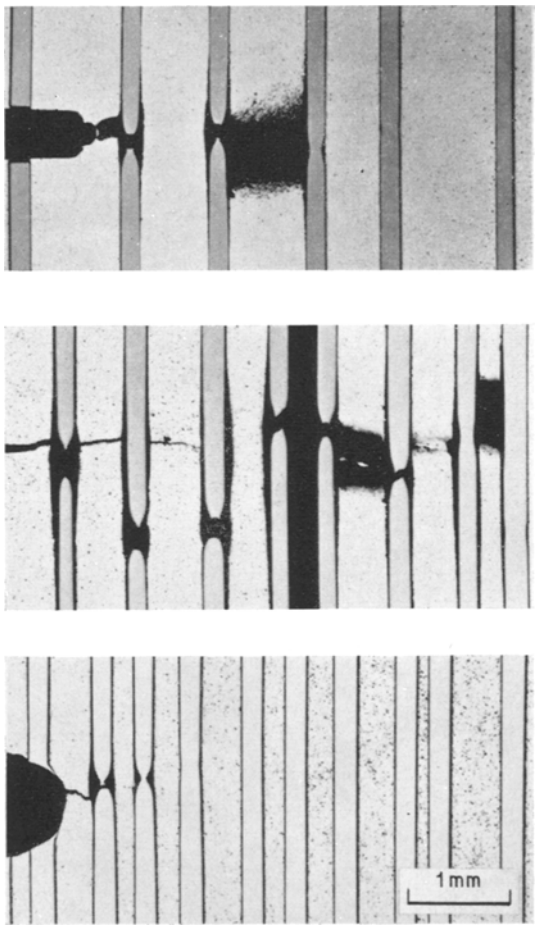

Figure 8 Crack path in 0.05, 0.10 and 0.20 volume fraction composites.

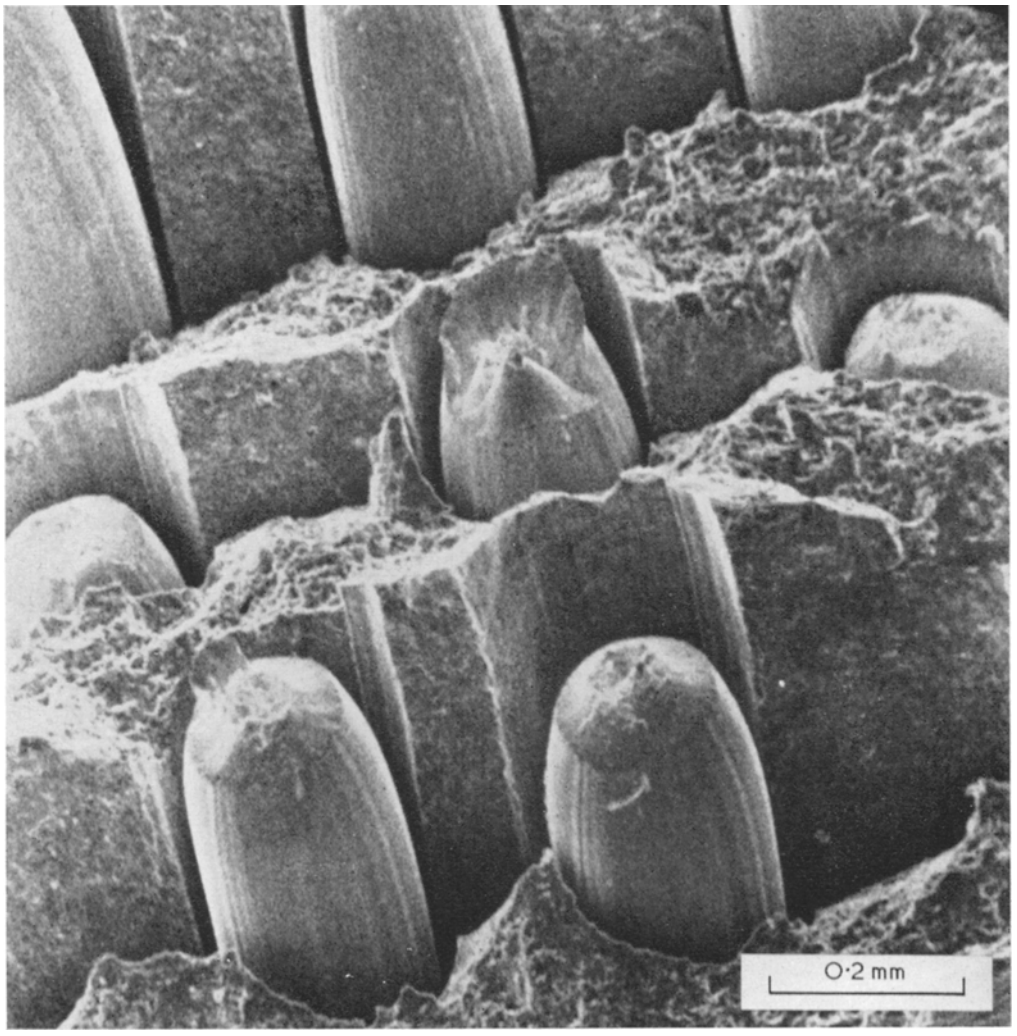

Figure 9 Scanning electron microscopy of 0.20 volume fraction fracture surface.

composites, the unloading path would actually be dependent upon both E_C and E_C' but the predominant term is E_C'. Moreover, in a separate study [21], the value of E_C' was successfully utilised to predict the displacement distribution and the critical stress intensity factor in these composites.

Next, consider a critical displacement criterion. The calculation of $2v_C^*$ from equations 9 and 15a is accomplished utilising the values of K, σ_{ys} and E_C' from table I. This gives a nearly constant value of $2v_C^*$ for all volume fractions and so it would appear that this is just as realistic a criterion as the fracture strain concept. This suggests that these two criteria may be equivalent. In fact, if one combines equations 9, 15a and 16, this leads to

$$2v_C^* = \pi l^* \epsilon^* , \tag{21}$$

which indicates that the critical crack-tip displacement is made up of a microstructural size parameter and a microstructural fracture strain. Using the observed values of l^* and ϵ_f from table I, an "observed" critical crack-tip displacement is determined from equation 21. In table II, this is seen to be in reasonable agreement with the calculated value of $2v_C^*$. Considering both criteria, there is little to choose between them since the statistical variation in the fracture strain is greater than any differences between observation and calculation. Even though one criterion might be as valid as the

TABLE I Observed fracture parameters

Volume fraction V_f	Stress** intensity K, kg mm$^{-\frac{3}{2}}$	No. of fibres in estimate	Yield strength σ_{ys}, kg mm^{-2}	Secondary modulus Ec', kg mm$^{-2} \times 10^{-3}$	Critical distance l^*, mm	Fracture strains, ϵ_f† range	average
0.05	196	3	52.5	1.19	0.104	(1.45-1.58)	1.52
0.10	262	7	69.6	2.58	0.157	(0.37-1.18)	0.72
0.10	289	8	69.6	2.58	0.145	(0.69-1.16)	0.94
0.20	518	2	93.0	4.66	0.145	(0.86-0.96)	0.91
0.20	434	1	93.0	4.66	0.173	(0.55)	0.55

**Average value for which fibre fractures were observed.
†Measured from diameters in micrographs using equation 18.

other, on pedagogical grounds alone, it seems preferable to lean to the critical fracture strain approach. That is, in less well-defined microstructures, the same critical crack-tip displacement could be made up of a large strain and a small structural size or a small strain and a large structural size. Thus, the flexibility of the two-parameter approach may be necessary to describe adequately the details of the fracture process.

Further substantiation of the overall approach was obtained where it was found [21] that the fibre contribution to the energy dissipation during fracture could be described by

$$G = 2d\,\epsilon^*\sigma_f V_f\,. \tag{22}$$

Here, $2d$ is the plastic strip height, which in this case happened to be about twice the fibre diameter. It may be shown that this is essentially equivalent to Rice's "plastic strip" model, which is discussed in the Appendix. From equations 15a and 22, it is seen that the stress intensity for crack propagation would be proportional to $(V_f)^{\frac{1}{2}}$ as long as the plastic strip was independent of the volume fraction. The data in table I substantiate this relationship approximately. Furthermore, since the product of the strain and plastic strip is approximately $2v_C$, then

$$G = 2v_C\sigma_f V_f\,, \tag{23}$$

which is essentially equation 12b considering a bulk material where the volume fraction is unity. To demonstrate this equivalence on experimental grounds, the average measured strain of 0.93 times $2d$ is equal to 0.43 mm while the average calculated value of $2v_C$ from table II is 0.52 mm. It should be pointed out that the plastic strip was actually found to be somewhat greater than $2d$ [21]. This, in conjunction with the fact that the average strain in the plastic strip would be somewhat less than σ_f, probably indicates why $2d\epsilon^*$ gives a reasonable estimate of the crack-tip displacement.§ In summary, it appears that both displacement and fracture strain criteria are valid ductile-fracture concepts as substantiated by fracture observations in a two-phase, ductile-fibrous composite. Additional experimental studies involving wide variations in volume fraction, shape, size and fracture-ductility of second phases must be run to enable further development of ductile-fracture criteria.

TABLE II Calculated and observed fracture criteria

Volume fraction V_f	Fracture strain		Critical crack-tip displacement	
	calculated ϵ^*	observed ϵ_f	calculated** $2v_c^*$, mm	observed† $2v_C^* = \pi l^* \epsilon_f$, mm
0.05	1.87	1.52	0.62	0.50
0.10	0.77	0.72	0.38	0.36
0.10	1.01	0.94	0.47	0.43
0.20	1.30	0.91	0.60	0.41
0.20	0.80	0.55	0.43	0.30
Average	1.15	0.93	0.50	0.40

**$2v_C^* = K^2/\sigma_{ys}E$ (combining equations 9 and 15a.)
†$2v_C^* = \pi l^* \epsilon^*$ (equation 21).
§It is emphasised that for some other fracture strain, such an agreement between the plastic strip and the fibre diameter would not necessarily be obtained. In fact, for a perfect agreement between equations 22 and 23, it is necessary for $\pi l^* = 2d$, which only occurs when $\epsilon^* = 0.90$, which happens to be the case here. Still, the analysis represented by equation 22 is valid for any fracture strain as long as the plastic strip height is properly assessed.

5. Conclusions

(i) A review of several fracture concepts indicates that both a single-parameter approach – utilising a critical crack-tip displacement, $2v_C^*$ – and a dual-parameter approach – utilising a structural size factor, l^*, and a critical fracture strain, ϵ^* – describe ductile-fracture at a crack-tip.

(ii) In an aluminium-matrix composite reinforced with unidirectional stainless-steel fibres, both of these models may be utilised as a fracture criterion to predict the critical displacement and/or fracture strain involved in fibre fracture at the crack-tip.

(iii) The statistical variation in the observed fracture strain of the fibres was greater than any differences between observation and theory.

(iv) Both theoretically and experimentally, it is shown that these two approaches are essentially equivalent, since the critical crack-tip displacement contains the other two parameters, i.e.

$$2v_C^* = \pi l^* \epsilon^* .$$

Nevertheless, the greater flexibility of the two-parameter approach is to be preferred for the description of the actual fracture process.

(v) It is demonstrated that an acoustic emission technique may be utilised to establish the point at which fibre fractures occur during the evaluation of a composite material.

(vi) If a composite material, with ductile unidirectional fibres, can be approximated by a "plastic-strip" model, then the stress intensity for crack propagation is proportional to $(V_f)^{\frac{1}{2}}$, V_f being the volume fraction of fibres.

Acknowledgement

The author would like to express his appreciation to Professor V. F. Zackay for helpful suggestions on the manuscript and to Dr D. Porter for the scanning electron microscopy.

This work was supported by the United States Atomic Energy Commission.

Appendix

Rice's [20] plastic strip model essentially simplifies the behaviour of real materials to one of a plastically-deforming strip of height, h, being pulled by two elastic slabs. Thus, as the crack propagates in the strip, only the strip deforms and the plastic zone is independent of crack length. Actually, this may approximate some real situations where, as the crack grows by a tearing action, the load drops so that a relatively constant stress intensity is maintained.

The strip model may then be used to determine the plastic energy dissipation rate as the plastic deformation extends from $x = l$ to $x = l + w$ by

$$\gamma_p = h \int_l^{l+w} \sigma_y \frac{\partial \epsilon_y{}^p}{\partial l} \, dx , \qquad (A1)$$

with σ_y being the stress and $\epsilon_y{}^p$ the plastic strain in the strip. If $\epsilon_y{}^p$ is only a function of the distance from the crack-tip $(x - l)$, then $\partial \epsilon_y{}^p / \partial x = -\partial \epsilon_y{}^p / \partial l$ and therefore from A1,

$$\gamma_p = h \int_{x=l+w}^{x=l} \sigma_y \, d\epsilon_y{}^p . \qquad (A2)$$

Thus, the plastic energy dissipation rate is given by the plastic strip height times the plastic strain energy density within the strip.

List of Symbols

A_0, A_f	initial, final cross-sectional areas
a_0	atomic spacing
B	specimen thickness
C	half-crack length
d	fibre diameter
E	Young's modulus
E_C	modulus of elasticity of composite
E_C'	secondary modulus of elasticity of composite
ϵ	strain adjacent to crack-tip
ϵ^*	fracture strain at crack-tip
ϵ_f	measured fracture strain
ξ_y	elastic shear strain
ξ^*	shear fracture strain at crack-tip
γ	work of fracture per unit fracture area
γ_s	surface tension
γ_p	plastic energy dissipation per unit fracture area
γ_m	effective energy absorption per unit fracture area $= \gamma_s + \gamma_p$
G	strain energy release rate $= 2\gamma_m$
$G_{I, III}$	G value appropriate to mode I, III
$K_{I, III}$	stress intensity factors appropriate to mode I, III
G_{Ic}, G_{IIIc}, K_{Ic}, K_{IIIc}	critical values at fracture
l	distance in front of crack
l^*	microstructural unit over which fracture occurs
P	externally applied load
ρ	crack-tip radius
R_p	plastic zone diameter
σ	externally applied stress
σ_C	theoretical strength of a solid
σ_{comp}	ultimate strength of a composite

$\sigma_{m,f}$	subscripts denoting matrix or fibre
σ_{ys}	uniaxial yield strength
τ_{ys}	shear yield strength
U	change of strain energy in a system with a flaw
μ	shear modulus
V	potential energy of creating fracture surface
$V_{m,f}$	volume fraction of matrix or fibres
v	displacement
v_c	crack-tip displacement
v_c^*	critical crack-tip displacement at fracture
v	Poisson's ratio
W	specimen width

References

1. A. H. COTTRELL, "The Tewkesbury Symposium on Fracture", edited by C. J. Osborn (Brown, Prior and Anderson Ltd, 1965) p. 1.
2. A. A. WELLS, *British Weld. J*, **10** (1965) 563.
3. A. S. TETELMAN and A. J. MCEVILY, "Fracture of Structural Materials" (John Wiley and Sons Inc, New York, 1967).
4. F. A. MCCLINTOCK, *Proc. Roy. Soc.* **285** (1965) 58.
5. F. A. MCCLINTOCK, S. M. KAPLAN, and C. A. BERG JR, *Internat. J. Fracture Mech.* **2** (1966) 614.
6. A. A. GRIFFITH, *Phil. Trans.* Ser. A **221** (1921) 163.
7. "Fracture, Microscopic and Macroscopic Fundamentals", Vol. 1, edited by H. Liebowitz (Academic Press Inc, New York, 1968).
8. A. S. TETELMAN and T. JOHNSTON, *Phil. Mag.* **11** (1965) 389.
9. E. OROWAN, *Trans. Inst. Eng. Shipbuild., Scotland* **89** (1945) 165.
10. G. R. IRWIN, "Fracturing of Metals" (ASM, Cleveland, 1948) p. 149.
11. B. A. BILBY, A. H. COTTRELL, and K. H. SWINDEN, *Proc. Roy. Soc.* Ser. A, **272** (1963) 304.
12. F. A. MCCLINTOCK and G. R. IRWIN, "Fracture Toughness Testing and Its Applications", ASTM STP 381 (Am. Soc. for Test. and Matls. Philadelphia, 1965) p. 84.
13. W. W. GERBERICH, *Experimental Mechanics*, November (1964) p. 335.
14. F. A. MCCLINTOCK, *ASTM Bulletin* April (1961) 277.
15. J. E. SRAWLEY and B. GROSS, *Materials Res. and Stnds.* 7 April (1967) 155.
16. V. F. ZACKAY, W. W. GERBERICH, and E. R. PARKER, "Fracture", Vol. 1, edited by H. Liebowitz (Academic Press Inc, New York, 1968) p. 395.
17. W. W. GERBERICH and C. E. HARTBOWER, "Fundamental Aspects of Stress Corrosion Cracking," edited by R. Staehle (National Assoc. of Corrosion Eng, Houston, 1969) p. 420.
18. W. W. GERBERICH, C. E. HARTBOWER, and P. P. CRIMMINS, *Weld. J. Res. Supp.* 47 No. 10 (1968) 433S.
19. "Aerospace Structural Metals Handbook", Vol. IIA, edited by V. Weiss and J. G. Sessler (Syracuse University Press, 1966) p. 3203.
20. J. R. RICE, Proceedings of the First International Conf. on Fracture, edited by Yokobori, Kawasaki and Swedlow (Japanese Soc. for Strength and Fracture of Materials, 1966) p. 309.
21. W. W. GERBERICH, Fracture in Metal-Metal Composites; Composite Materials Fundamentals and Utilization (University of California, Berkeley, June 1968).

Received 23 October 1968 and accepted 6 January 1970.